Available online at www.sciencedirect.com

ScienceDirect

Procedia Structural Integrity 33 (2021) 287–294

Structural Integrity Procedia

www.elsevier.com/locate/procedia

IGF26 - 26th International Conference on Fracture and Structural Integrity

On the thermal response of LuAG:Ce single crystals

George Saatsakis[a], Dionysios Linardatos[a], George Karpetas[b], Nektarios Kalyvas[a], Konstantinos Ninos[c], Athanasios Bakas[c], Eleftherios Lavdas[c], George Fountos[a], Ioannis Kandarakis[a], IoannisValais[a] and Christos Michail[a],*

[a]*University of West Attica, Radiation Physics, Materials Technology and Biomedical Imaging Laboratory, Department of Biomedical Engineering, Athens 12210, Greece*

[b]*University of Thessaly, Department of Medical Physics, Faculty of Medicine, Larissa 41110,Greece*

[c]*University of West Attica, Department of Biomedical Sciences, Athens 12210, Greece*

Abstract

It is well known that the luminescence efficiency of single crystals is affected by external parameters, such as the environmental temperature, especially in harsh environments. Due to this, it is of worth to examine the influence of temperature on the luminescence output of single-crystal scintillators. In this study lutetium aluminum garnet ($Lu_3Al_5O_{12}$:Ce-LuAG:Ce) was examined, against previously published data for cadmium tungstate ($CdWO_4$) and calcium fluoride doped with europium (CaF_2:Eu) single crystals. Experiments were carried using a medical X-ray source, set to fixed high voltage (90kVp) and tube current/exposure time product (63mAs), in order to record the produced light, under different temperature conditions (20-120 Celsius). An interesting finding is that temperature, in the examined range, appear to have minimal influence on the light output of LuAG:Ce, in the contrary to the previously examined crystals ($CdWO_4$ and CaF_2:Eu) where the luminescence output constantly decreased with increasing temperature. The thermal stability of LuAG:Ce, in the examined temperature range, renders it a good choice, besides medical imaging, also for application in harsh environments as well as for long-term operation in high power LEDs.

Keywords: Radiation detectors; Single Crystals; $Lu_3Al_5O_{12}$:Ce; $CdWO_4$, CaF_2:Eu, Temperature dependence

* Corresponding author. Tel.: +30-210-538-5387.
E-mail address: cmichail@uniwa.gr

10.1016/j.prostr.2021.10.035

1. Introduction

Radiation converters (Kandarakis, 2016), are frequently tailor-made for application in non-destructive testing (NDT), medical imaging, high energy experiments, optoelectronics, at harsh environments, well-logging, etc. (Kytyr et al., 2011; Linardatos et al., 2020; Mares et al., 2012; Martini et al., 2018, 2019, 2020; Michail et al., 2016a, 2018a; Mykhaylyk et al., 2019; Yanagida et al., 2013). Well known scintillators are NaI, CsI, GSO, BGO, LSO, etc. (Eijk, 2002; Karpetas et al., 2017; Melcher et al., 1991; Michail et al., 2016b). When used in harsh applications, parameters such as radiation or temperature alters their luminescence response (Bisong et al., 2019; Bulatovic et al., 2013; Lebedev et al., 2019; Melcher et al., 1991; Patri et al., 2019; Rothkirch et al., 2013; Saxena, 2019). Thus, it is required careful selection of their intrinsic properties (Yang et al., 2014).

An interesting crystal scintillator is $Lu_3Al_5O_{12}$, activated by cerium (Ce) (LuAG:Ce) (Hu et al., 2020; Witkiewicz-Lukaszek et al., 2018). $Lu_3Al_5O_{12}$:Ce is a promising relatively new material that has been examined for various applications (Chewpraditkul et al., 2009; Chewpraditkul and Moszynski, 2011; Gundacker et al., 2016; Lucchini et al., 2018, 2016; Sreebunpeng et al., 2017). The density is 6.73 g/cm^3, and the light yield data, published in the literature, range from 16700 to 27000 photons/MeV (Li et al., 2005; Liu et al., 2016; Mares et al., 2012; Nikl et al., 2016; Sreebunpeng et al., 2017). The emission maximum is at 535 nm (Nikl et al., 2013; Ogiegło et al., 2013). The scintillation response is at 69 ns (Swiderski et al., 2009, p. 3). LuAG:Ce energy resolution range is 6.5% at 662 keV (Swiderski et al., 2009) and the refractive index is 1.84 (Kobayashi et al., 2012). The thermal conductivity has been reported at 9.6 W m^{-1} K^{-1}, the specific heat is 0.411 J g^{-1} K^{-1} and the thermal expansion coefficient is 8.8x10^{-6} (C^{-1}) (Brylew et al., 2013; Kastengren, 2019; Kuwano et al., 2004). LuAG:Ce has been also studied for optoelectronic applications in light emitting diodes (LEDs) and for electromagnetic calorimetry (Derdzyan et al., 2012; Ivanovskikh et al., 2012; Mares et al., 2012; Nikl et al., 2016; Zorenko et al., 2017).

In this article, experimental data on the luminescence output of LuAG:Ce are reported and compared against previously published data for $CdWO_4$ and CaF_2:Eu crystals with increasing temperature (Rutherford et al., 2016; Saatsakis et al., 2020b).

$CdWO_4$ (one of the most widely applied scintillators for various applications) (Ziluei et al., 2017) and CaF_2:Eu have high melting points at 1325°C ($CdWO_4$), and 1360°C (CaF_2:Eu) and are robust to mechanical and thermal shocks, which are essential properties for extreme environmental applications (Wang et al., 2018). Their properties are shown in Table 1 (Chen, 2008; Dujardin et al., 2018; Eijk, 2002; Eritenko and Tsvetyansky, 2020; Fan et al., 2018; Galashov et al., 2014; Lecoq, 2016; Lecoq et al., 2017; Michail et al., 2020; Ruiz-Fuertes et al., 2017; Saatsakis et al., 2020a; Ziluei et al., 2017). In previous studies of our group, the luminescence efficiency was measured under typical medical X-ray conditions.

Table 1. Comparison of LuAG:Ce, $CdWO_4$ and CaF_2:Eu properties (Christos Michail et al., 2020; C. Michail et al., 2020; Michail et al., 2019).

		Crystal material		
		$Lu_3Al_5O_{12}$:Ce	$CdWO_4$	CaF_2:Eu
Properties Mechanical	Units	Value		
Density	g/cm³	6.73	7.9	3.18
Atomic Number (Effective)		62.9	61-66	16.5
Melting Point	ºK	2020	1325	1360
Linear Expansion Coeff.	C^{-1}	8.8 x10^{-6}	10.2x10^{-6}	19.5 x 10^{-6}
Thermal Conductivity	$Wm^{-1}K^{-1}$	9.6	4.69(@300K)	9.7
Hardness	Mho	8.5	4-4.5	4
Emission maximum (nm)	nm	535	490	435

2. Materials and Methods

All the examined crystal samples (namely LuAG:Ce, $CdWO_4$ and CaF_2:Eu) have polished surfaces with equal dimensions (10x10x10mm) (Advatech, 2020). They were irradiated using a BMI General Medical Merate tube (90 kVp and 63mAs) in order to measure the light photon intensity dependence with temperature (20 to 120 °C). The X-ray beam was filtered with an external aluminium filter (2cm), simulating the beam quality alteration by a typical human chest (Michail et al., 2018b). The crystal sample was heated up to 120°, using a Perel 3700-9 2000W heating gun. The temperature on the crystal surface was monitored using an Extech RH101 infrared digital thermometer (0.1% accuracy).

2.1. Luminescence Efficiency

The light flux emitted by the crystal samples upon X-ray irradiation was measured, by placing the crystals at the upper port of an integrating sphere (Oriel 70451) coupled at the output port with a photomultiplier (PMT) (EMI 9798B) (Saatsakis et al., 2020a). The photomultiplier's photocathode (extended S-20) signal was fed to a Sub-Femtoamp electrometer (Keithley, 6430) (Saatsakis et al., 2019). This set-up was used to measure electrometer's electric current to estimate the light flux $\dot{\Psi}_\lambda$:

$$\dot{\Psi}_\lambda = \frac{I_{elec}}{\tau_0(s_{PC}a_s)} \cdot \frac{1}{A_{sc}} \tag{2.1}$$

Parameters I_{elec}, s_{PC}, α_S, A_{sc} and τ_0 were defined in previous publications (Saatsakis et al., 2020a).

Then the light output over the X-ray exposure rate of the crystals was calculated as (Michail et al., 2019):

$$\eta_A = \dot{\Psi}_\lambda / \dot{X} \tag{2.2}$$

Where $\dot{X}$ is the exposure rate incident on the crystal. Efficiency-units (EU) are expressed in $\mu W \times m^{-2} /(mR \times s^{-1})$. The S.I. equivalent is $\mu W \times m^{-2} /(mGy \times s^{-1})$, where mGy is the corresponding air Kerma.

3. Results and Discussion

Figure 1 shows the variation of PMT normalized output voltage values (the electrometer sensing voltage was below 1Vpp) for the LuAG:Ce crystal, with exposure time and temperature. The shape of the curves presented in Fig.1, illustrate the exposure of LuAG:Ce crystal to the X-rays emitted from the X-ray tube. As it can be seen in X-ray exposure, between 0.0 and 0.4 sec there is a rapid increase of X-ray photons, reaching a plateau between 0.5 and 1 sec and then a rapid decrease (1 sec to 1.2 sec).

The output is relatively stable in the examined temperature range. This finding is clearly depicted in Fig. 2, which shows the luminescence output of LuAG:Ce, compared to previously studied scintillation crystals of similar dimensions, i.e. $CdWO_4$ and CaF_2:Eu, at a temperature range from 20 to 120 °C (AE 26.3 at 20 °C to 26.9 at 120 °C). The latter is an indicative temperature range that can be found in logging detectors in which crystals are subjected to temperatures in the range from minus 0 °C to more than 200 °C or long-lasting optoelectronic devices (Hu et al., 2015; Melcher et al., 1991; Onderisinova et al., 2015; Xiang et al., 2016). Exposure of the scintillator to excessive heating or X-ray flux can result in crystal cracking (Kastengren, 2019; Pokluda et al., 2015).

This finding is in accordance with previously published works for LuAG:Ce in which, as the temperature was increased, the light output of LuAG:Ce sample degraded less than 9%, compared to that at room temperature (Hu et al., 2015; Onderisinova et al., 2015; Xiang et al., 2016) showing the improved thermal quenching behavior of this material for high power phosphor-converted WLEDs. In the work of Herzog et al. (2020), LuAG:Ce was also found stable in this temperature range (Herzog et al., 2020). The thermal quenching behavior of LuAG:Ce was previously examined and was found significantly better than other well-known scintillators (Chen et al., 2010; Xu et al., 2018). Furthermore, LuAG:Ce in ceramic form was reported with about 3% intensity drop after 1000 h, at 85 °C and 85% humidity and thermal quenching with reduction of about 3% at 200 °C (Ji et al., 2015; Xu et al., 2018). According to Xu et al., the drop, as response to temperature increase, is directly related to the lattice vibration, which often provides the activation energy for non-radiative transitions (Xu et al., 2018). On the other hand the luminescence efficiency of $CdWO_4$ and CaF_2:Eu constantly decreased, with increasing temperature, for both crystals due to thermal quenching (Melcher et al., 1991). The luminescence signal was found in both crystals maximum at the lowest examined temperature (23.06 E.U. for $CdWO_4$ and 22.01 E.U. for CaF_2:Eu at 22 °C). In the mid-temperature range (50-80 °C) $CdWO_4$ shows increased differences compared to CaF_2:Eu (Saatsakis et al., 2020a, 2020b).

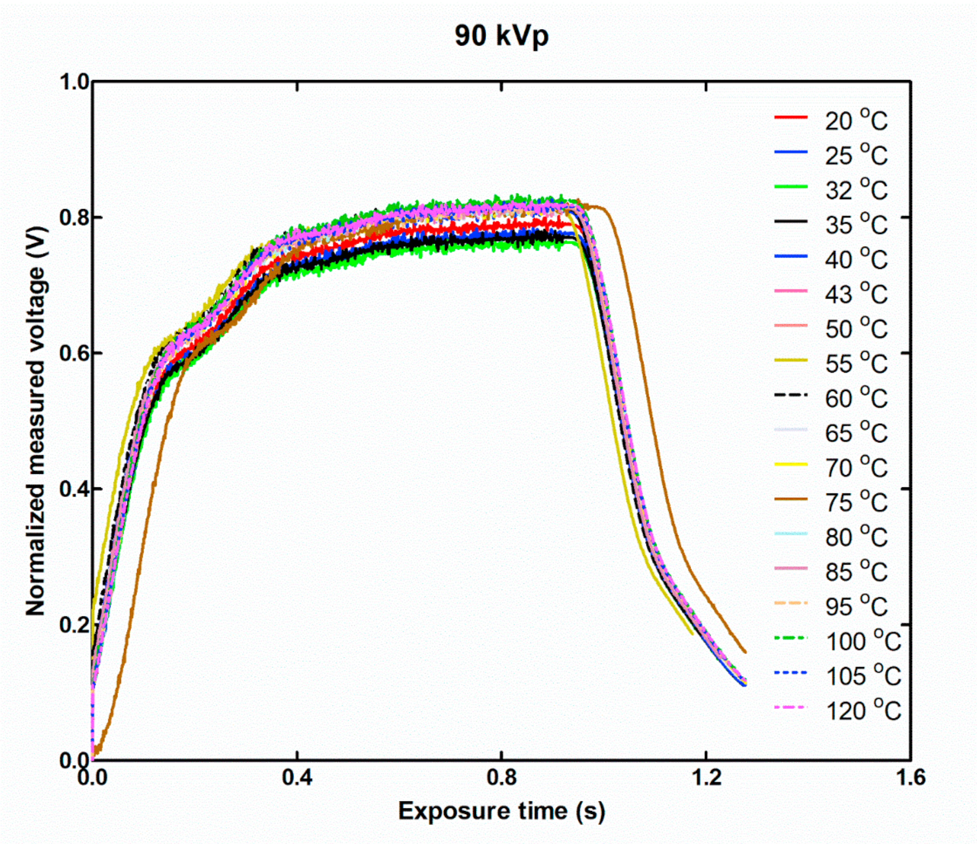

Fig. 1. PMT normalized output voltage values for the LuAG:Ce crystal, with exposure time and temperature.

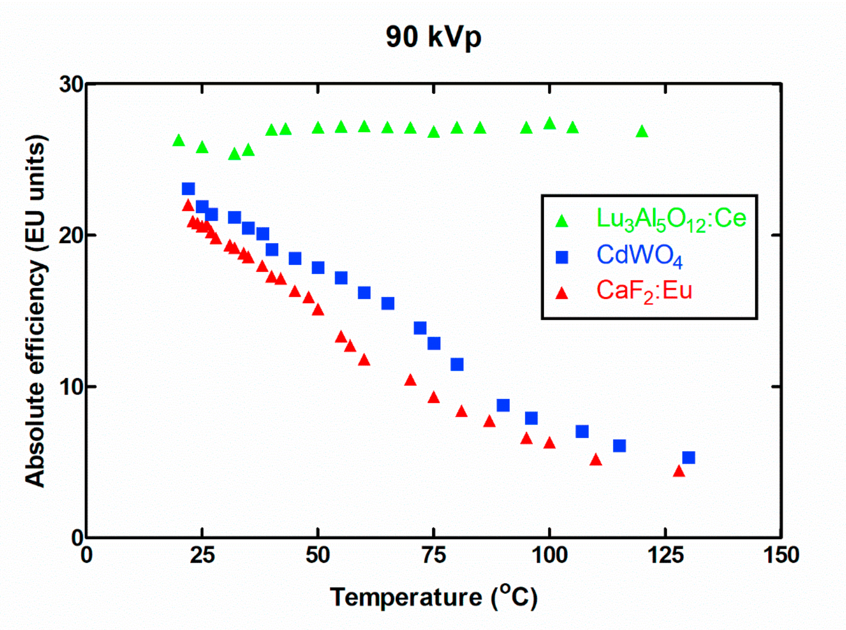

Fig. 2. Comparison between the luminescence efficiency of the examined single crystals in the temperature range from 22 to 120º C.

4. Conclusions

In this research, the effect of temperature on the luminescence output of LuAG:Ce, $CdWO_4$ and CaF_2:Eu single crystals, for applications in harsh environments and optoelectronics, was examined. The luminescence output values of LuAG:Ce were found stable in this temperature range, in contrast to CdWO4 and CaF_2:Eu which showed a decrease down to 77-79% when the crystal surfaces were heated to the maximum operating temperature. The thermal stability of LuAG:Ce, in the examined temperature range, renders it a good choice for application in harsh environments as well as for long-term operation in high power LEDs.

References

Advatech UK. Radiation Detectors and Sensors. Available online: https://www.advatech-uk.co.uk/radiationdetectors-scint.html (accessed on 01-06-2021).

Bisong, M.S., Mikhailov, V.E., Lepov, V.V., Makharova, S.N., 2019. Microstructure influence on crack resistance of steels welded structures operated in an extremely cold environment. Procedia Structural Integrity, 1st International Conference on Integrity and Lifetime in Extreme Environment (ILEE-2019) 20, 37–41. https://doi.org/10.1016/j.prostr.2019.12.112

Brylew, K., Drozdowski, W., Witkowski, M.E., Kamada, K., Yanagida, T., Yoshikawa, A., 2013. Effect of thermal annealing in air on scintillation properties of LuAG and LuAG:Pr. centr.eur.j.phys. 11, 138–142. https://doi.org/10.2478/s11534-012-0153-5

Bulatovic, S., Aleksic, V., Milovic, L., 2013. Failure of steam line causes determined by NDT testing in power and heating plants. Fra&IntStrut 7, 41–48. https://doi.org/10.3221/IGF-ESIS.26.05

Chen, L., Lin, C.-C., Yeh, C.-W., Liu, R.-S., 2010. Light Converting Inorganic Phosphors for White Light-Emitting Diodes. Materials 3, 2172–2195. https://doi.org/10.3390/ma3032172

Chen, M.C., 2008. Double beta decay: Scintillators. J. Phys.: Conf. Ser. 136, 022035. https://doi.org/10.1088/1742-6596/136/2/022035

Chewpraditkul, W., Swiderski, L., Moszynski, M., Szczesniak, T., Syntfeld-Kazuch, A., Wanarak, C., Limsuwan, P., 2009. Scintillation Properties of LuAG:Ce, YAG:Ce and LYSO:Ce Crystals for Gamma-Ray Detection. IEEE Transactions on Nuclear Science 56, 3800–3805. https://doi.org/10.1109/TNS.2009.2033994

Chewpraditkul, W., Moszynski, M., 2011. Scintillation Properties of $Lu_3Al_5O_{12}$, Lu_2SiO_5 and $LaBr_3$ Crystals Activated with Cerium. Physics Procedia, 2011 International Conference on Physics Science and Technology (ICPST 2011) 22, 218–226.

https://doi.org/10.1016/j.phpro.2011.11.035
Derdzyan, M.V., Ovanesyan, K.L., Petrosyan, A.G., Belsky, A., Dujardin, C., Pedrini, C., Auffray, E., Lecoq, P., Lucchini, M., Pauwels, K., 2012. Radiation hardness of LuAG:Ce and LuAG:Pr scintillator crystals. Journal of Crystal Growth 361, 212–216. https://doi.org/10.1016/j.jcrysgro.2012.09.046
Dujardin, C., Auffray, E., Bourret-Courchesne, E., Dorenbos, P., Lecoq, P., Nikl, M., Vasil'ev, A.N., Yoshikawa, A., Zhu, R.-, 2018. Needs, Trends, and Advances in Inorganic Scintillators. IEEE Transactions on Nuclear Science 65, 1977–1997. https://doi.org/10.1109/TNS.2018.2840160
Eijk, C.W.E. van, 2002. Inorganic scintillators in medical imaging. Phys. Med. Biol. 47, R85–R106. https://doi.org/10.1088/0031-9155/47/8/201
Eritenko, A.N., Tsvetyansky, A.L., 2020. Separation of materials according to the effective atomic number using photons of two energies in the range of 60–700 keV. Nuclear Instruments and Methods in Physics Research Section B: Beam Interactions with Materials and Atoms 462, 114–118. https://doi.org/10.1016/j.nimb.2019.10.020
Fan, T., Lü, J., Huang, Y., Li, G., 2018. Monodispersing Eu^{3+} and Li^{+} codoped CaF_2 nanoparticles for efficient luminescence. Micro & Nano Letters 13, 393–396. https://doi.org/10.1049/mnl.2017.0662
Galashov, E.N., Atuchin, V.V., Kozhukhov, A.S., Pokrovsky, L.D., Shlegel, V.N., 2014. Growth of $CdWO_4$ crystals by the low thermal gradient Czochralski technique and the properties of a (010) cleaved surface. Journal of Crystal Growth, Proceedings of 17th International Conference on Crystal Growth and Epitaxy (ICCGE-17) 401, 156–159. https://doi.org/10.1016/j.jcrysgro.2014.01.029
Gundacker, S., Acerbi, F., Auffray, E., Ferri, A., Gola, A., Nemallapudi, M.V., Paternoster, G., Piemonte, C., Lecoq, P., 2016. State of the art timing in TOF-PET detectors with LuAG, GAGG and L(Y)SO scintillators of various sizes coupled to FBK-SiPMs. J. Inst. 11, P08008–P08008. https://doi.org/10.1088/1748-0221/11/08/P08008
Herzog, J.M., Witkowski, D., Rothamer, D.A., 2020. Combustion-relevant aerosol phosphor thermometry imaging using Ce,Pr:LuAG, Ce:$GdPO_4$, and Ce:CSSO. Proceedings of the Combustion Institute. https://doi.org/10.1016/j.proci.2020.06.193
Hu, C., Liu, S.-P., Fasoli, M., Vedda, A., Nikl, M., Feng, X.-Q., Pan, Y.-B., 2015. ESR and TSL study of hole and electron traps in LuAG:Ce,Mg ceramic scintillator. Optical Materials 45, 252–257. https://doi.org/10.1016/j.optmat.2015.03.049
Hu, C., Li, J., Yang, F., Jiang, B., Zhang, L., Zhu, R.-Y., 2020. LuAG ceramic scintillators for future HEP experiments. Nuclear Instruments and Methods in Physics Research Section A: Accelerators, Spectrometers, Detectors and Associated Equipment, Symposium on Radiation Measurements and Applications XVII 954, 161723. https://doi.org/10.1016/j.nima.2018.12.038
Ivanovskikh, K.V., Ogiegło, J.M., Zych, A., Ronda, C.R., Meijerink, A., 2012. Luminescence Temperature Quenching for Ce^{3+} and Pr^{3+} d-f Emission in YAG and LuAG. ECS J. Solid State Sci. Technol. 2, R3148. https://doi.org/10.1149/2.011302jss
Ji, E.-K., Song, Y.-H., Bak, S.H., Jung, M.K., Jeong, B.W., Lee, D.B., Yoon, D.-H., 2015. The design of a ceramic phosphor plate with functional materials for application in high power LEDs. J. Mater. Chem. C 3, 12390–12393. https://doi.org/10.1039/C5TC02795K
Kandarakis, I.S., 2016. Luminescence in medical image science. Journal of Luminescence, The 17th International Conference on Luminescence and Optical Spectroscopy of Condensed Matter (ICL'14) 169, 553–558. https://doi.org/10.1016/j.jlumin.2014.11.009
Karpetas, G.E., Michail, C.M., Fountos, G.P., Kalyvas, N.I., Valais, I.G., Kandarakis, I.S., Panayiotakis, G.S., 2017. Detective quantum efficiency (DQE) in PET scanners: A simulation study. Applied Radiation and Isotopes 125, 154–162. https://doi.org/10.1016/j.apradiso.2017.04.018
Kastengren, A., 2019. Thermal behavior of single-crystal scintillators for high-speed X-ray imaging. J Synchrotron Rad 26, 205–214. https://doi.org/10.1107/S1600577518015230
Kobayashi, M., Aogaki, S., Takeutchi, F., Tamagawa, Y., Usuki, Y., 2012. Performance of thin long scintillator strips of GSO:Ce, LGSO:Ce and LuAG:Pr for low energy γ-rays. Nuclear Instruments and Methods in Physics Research Section A: Accelerators, Spectrometers, Detectors and Associated Equipment 693, 226–235. https://doi.org/10.1016/j.nima.2012.07.045
Kuwano, Y., Suda, K., Ishizawa, N., Yamada, T., 2004. Crystal growth and properties of $(Lu,Y)_3Al_5O_{12}$. Journal of Crystal Growth 260, 159–165. https://doi.org/10.1016/j.jcrysgro.2003.08.060
Kytyr, D., Doktor, T., Jirousek, O., Zlamal, P., Pokorny, D., 2011. Experimental and numerical study of cemented bone-implant interface behavior. Fra&IntStrut 5, 5–13. https://doi.org/10.3221/IGF-ESIS.15.01
Lebedev, M.P., Startsev, O.V., Kychkin, A.K., 2019. Development of climatic tests of polymer materials for extreme operating conditions. Procedia Structural Integrity, 1st International Conference on Integrity and Lifetime in Extreme Environment (ILEE-2019) 20, 81–86. https://doi.org/10.1016/j.prostr.2019.12.119
Lecoq, P., 2016. Development of new scintillators for medical applications. Nuclear Instruments and Methods in Physics Research Section A: Accelerators, Spectrometers, Detectors and Associated Equipment, Advances in detectors and applications for medicine 809, 130–139. https://doi.org/10.1016/j.nima.2015.08.041
Lecoq, P., Gektin, A., Korzhik, M., 2017. Inorganic Scintillators for Detector Systems: Physical Principles and Crystal Engineering, 2nd ed, Particle Acceleration and Detection. Springer International Publishing. https://doi.org/10.1007/978-3-319-45522-8
Li, H.-L., Liu, X.-J., Huang, L.-P., 2005. Fabrication of Transparent Cerium-Doped Lutetium Aluminum Garnet (LuAG:Ce) Ceramics by a Solid-State Reaction Method. Journal of the American Ceramic Society 88, 3226–3228. https://doi.org/10.1111/j.1551-2916.2005.00554.x
Linardatos, D., Konstantinidis, A., Valais, I., Ninos, K., Kalyvas, N., Bakas, A., Kandarakis, I., Fountos, G., Michail, C., 2020. On the Optical Response of Tellurium Activated Zinc Selenide ZnSe:Te Single Crystal. Crystals 10, 961. https://doi.org/10.3390/cryst10110961
Liu, S., Feng, X., Mares, J.A., Babin, V., Nikl, M., Beitlerova, A., Shi, Y., Zeng, Y., Pan, Y., D'Ambrosio, C., Huang, Y., 2016. Optical, luminescence and scintillation characteristics of non-stoichiometric LuAG:Ce ceramics. Journal of Luminescence 169, 72–77. https://doi.org/10.1016/j.jlumin.2015.08.034
Lucchini, M.T., Pauwels, K., Blazek, K., Ochesanu, S., Auffray, E., 2016. Radiation Tolerance of LuAG:Ce and YAG:Ce Crystals Under High Levels of Gamma- and Proton-Irradiation. IEEE Transactions on Nuclear Science 63, 586–590. https://doi.org/10.1109/TNS.2015.2493347
Lucchini, M.T., Buganov, O., Auffray, E., Bohacek, P., Korjik, M., Kozlov, D., Nargelas, S., Nikl, M., Tikhomirov, S., Tamulaitis, G., Vaitkevicius, A., Kamada, K., Yoshikawa, A., 2018. Measurement of non-equilibrium carriers dynamics in Ce-doped YAG, LuAG and GAGG crystals with and without Mg-codoping. Journal of Luminescence 194, 1–7. https://doi.org/10.1016/j.jlumin.2017.10.005
Mares, J.A., Nikl, M., Beitlerova, A., Horodysky, P., Blazek, K., Bartos, K., D'Ambrosio, C., 2012. Scintillation Properties of Ce^{3+} and Pr^{3+} -Doped

LuAG, YAG and Mixed $Lu_xY_{1-x}AG$ Garnet Crystals. IEEE Transactions on Nuclear Science 59, 2120–2125. https://doi.org/10.1109/TNS.2012.2191573

Martini, N., Koukou, V., Fountos, G., Valais, I., Bakas, A., Ninos, K., Kandarakis, I., Panayiotakis, G., Michail, Ch., 2018. Towards the enhancement of medical imaging with non-destructive testing (NDT) CMOS sensors. Evaluation following IEC 62220-1-1:2015 international standard. Procedia Structural Integrity 10, 326–332. https://doi.org/10.1016/j.prostr.2018.09.045

Martini, N., Koukou, V., Fountos, G., Valais, I., Kandarakis, I., Michail, C., Bakas, A., Lavdas, E., Ninos, K., Oikonomou, G., Gogou, L., Panayiotakis, G., 2019. Imaging performance of a $CaWO_4$/CMOS sensor. Frattura ed Integrità Strutturale 13, 471–480. https://doi.org/10.3221/IGF-ESIS.50.39

Martini, N., Koukou, V., Michail, C., Fountos, G., 2020. Dual Energy X-ray Methods for the Characterization, Quantification and Imaging of Calcification Minerals and Masses in Breast. Crystals 10, 198. https://doi.org/10.3390/cryst10030198

Melcher, C.L., Schweitzer, J.S., Manente, R.A., Peterson, C.A., 1991. Applications of single crystals in oil well logging. Journal of Crystal Growth 109, 37–42. https://doi.org/10.1016/0022-0248(91)90155-X

Michail, C., Valais, I., Martini, N., Koukou, V., Kalyvas, N., Bakas, A., Kandarakis, I., Fountos, G., 2016a. Determination of the detective quantum efficiency (DQE) of CMOS/CsI imaging detectors following the novel IEC 62220-1-1:2015 International Standard. Radiation Measurements 94, 8–17. https://doi.org/10.1016/j.radmeas.2016.04.005

Michail, C., Karpetas, G.E., Fountos, G.P., Kalyvas, N.I., Valais, I.G., Fountzoula, C., Zanglis, A., Kandarakis, I.S., Panayiotakis, G.S., 2016b. A novel method for the optimization of positron emission tomography scanners imaging performance. Hell J Nucl Med 19, 231–240. https://doi.org/10.1967/s002449910405

Michail, C., Karpetas, G., Kalyvas, N., Valais, I., Kandarakis, I., Agavanakis, K., Panayiotakis, G., Fountos, G., 2018a. Information Capacity of Positron Emission Tomography Scanners. Crystals 8, 459. https://doi.org/10.3390/cryst8120459

Michail, C., Valais, I., Fountos, G., Bakas, A., Fountzoula, C., Kalyvas, N., Karabotsos, A., Sianoudis, I., Kandarakis, I., 2018b. Luminescence efficiency of calcium tungstate ($CaWO_4$) under X-ray radiation: Comparison with Gd_2O_2S:Tb. Measurement 120, 213–220. https://doi.org/10.1016/j.measurement.2018.02.027

Michail, C., Kalyvas, N., Bakas, A., Ninos, K., Sianoudis, I., Fountos, G., Kandarakis, I., Panayiotakis, G., Valais, I., 2019. Absolute Luminescence Efficiency of Europium-Doped Calcium Fluoride (CaF_2:Eu) Single Crystals under X-ray Excitation. Crystals 9, 234. https://doi.org/10.3390/cryst9050234

Michail, C., Koukou, V., Martini, N., Saatsakis, G., Kalyvas, N., Bakas, A., Kandarakis, I., Fountos, G., Panayiotakis, G., Valais, I., 2020a. Luminescence Efficiency of Cadmium Tungstate ($CdWO_4$) Single Crystal for Medical Imaging Applications. Crystals 10, 429. https://doi.org/10.3390/cryst10060429

Michail, C., Ninos, K., Kalyvas, N., Bakas, A., Saatsakis, G., Fountos, G., Sianoudis, I., Panayiotakis, G., Kandarakis, I., Valais, I., 2020b. Spectral efficiency of lutetium aluminum garnet ($Lu_3Al_5O_{12}$:Ce) with microelectronic optical sensors. Microelectronics Reliability 109, 113658. https://doi.org/10.1016/j.microrel.2020.113658

Mykhaylyk, V.B., Kraus, H., Saliba, M., 2019. Bright and fast scintillation of organolead perovskite $MAPbBr_3$ at low temperatures. Mater. Horiz. 6, 1740–1747. https://doi.org/10.1039/C9MH00281B

Nikl, M., Babin, V., Mares, J.A., Kamada, K., Kurosawa, S., Yoshikawa, A., Tous, J., Houzvicka, J., Blazek, K., 2016. The role of cerium variable charge state in the luminescence and scintillation mechanism in complex oxide scintillators: The effect of air annealing. Journal of Luminescence, The 17th International Conference on Luminescence and Optical Spectroscopy of Condensed Matter (ICL'14) 169, 539–543. https://doi.org/10.1016/j.jlumin.2015.01.008

Nikl, M., Yoshikawa, A., Kamada, K., Nejezchleb, K., Stanek, C.R., Mares, J.A., Blazek, K., 2013. Development of LuAG-based scintillator crystals – A review. Progress in Crystal Growth and Characterization of Materials 59, 47–72. https://doi.org/10.1016/j.pcrysgrow.2013.02.001

Ogiegło, J.M., Zych, A., Jüstel, T., Meijerink, A., Ronda, C.R., 2013. Luminescence and energy transfer in $Lu_3Al_5O_{12}$ scintillators co-doped with Ce^{3+} and Pr^{3+}. Optical Materials 35, 322–331. https://doi.org/10.1016/j.optmat.2012.08.010

Onderisinova, Z., Kucera, M., Hanus, M., Nikl, M., 2015. Temperature-dependent nonradiative energy transfer from Gd^{3+} to Ce^{3+} ions in co-doped LuAG:Ce,Gd garnet scintillators. Journal of Luminescence 167, 106–113. https://doi.org/10.1016/j.jlumin.2015.06.014

Patri, S., Kumar, H., Prasad, K.K., Meikandamurthy, C., Sreedhar, B.K., Vijayashree, R., Prakash, V., Selvaraj, P., 2019. Failure analysis of structural screw joint in a start-up neutron detector handling mechanism. Procedia Structural Integrity, SICE 2018 (2nd International Conference on Structural Integrity and Exhibition 2018) 14, 688–695. https://doi.org/10.1016/j.prostr.2019.05.086

Pokluda, J., Vojtek, T., Hohenwarter, A., Pippan, R., 2015. Effects of microstructure and crystallography on crack path and intrinsic resistance to shear-mode fatigue crack growth. Fra&IntStrut 9. https://doi.org/10.3221/IGF-ESIS.34.15

Rothkirch, A., Gatta, G.D., Meyer, M., Merkel, S., Merlini, M., Liermann, H.-P., 2013. Single-crystal diffraction at the Extreme Conditions beamline P02.2: procedure for collecting and analyzing high-pressure single-crystal data. J Synchrotron Rad 20, 711–720. https://doi.org/10.1107/S0909049513018621

Ruiz-Fuertes, J., Friedrich, A., Errandonea, D., Segura, A., Morgenroth, W., Rodríguez-Hernández, P., Muñoz, A., Meng, Y., 2017. Optical and structural study of the pressure-induced phase transition of $CdWO_4$. Phys. Rev. B 95, 174105. https://doi.org/10.1103/PhysRevB.95.174105

Rutherford, M.E., Chapman, D.J., White, T.G., Drakopoulos, M., Rack, A., Eakins, D.E., 2016. Evaluating scintillator performance in time-resolved hard X-ray studies at synchrotron light sources. J Synchrotron Rad 23, 685–693. https://doi.org/10.1107/S1600577516002770

Saatsakis, G., Kalyvas, N., Michail, C., Ninos, K., Bakas, A., Fountzoula, C., Sianoudis, I., Karpetas, G.E., Fountos, G., Kandarakis, I., Valais, I., Panayiotakis, G., 2019. Optical Characteristics of ZnCuInS/ZnS (Core/Shell) Nanocrystal Flexible Films under X-Ray Excitation. Crystals 9, 343. https://doi.org/10.3390/cryst9070343

Saatsakis, G., Linardatos, D., Ninos, K., Valais, I., Kalyvas, N., Bakas, A., Kandarakis, I., Fountos, G., Panayiotakis, G., Michail, C., 2020a. Temperature Dependence of the Luminescence output of CdWO4 Crystal. Comparison with CaF_2:Eu. Procedia Structural Integrity, 1st Virtual European Conference on Fracture - VECF1 28, 971–977. https://doi.org/10.1016/j.prostr.2020.11.071

Saatsakis, G., Ninos, K., Valais, I., Martini, N., Kalyvas, N., Kantsos, C., Bakas, A., Kandarakis, I., Panayiotakis, G., Michail, C., 2020b. Luminescence efficiency of CaF_2:Eu single crystals: Temperature dependence. Procedia Structural Integrity 26, 3–10.

https://doi.org/10.1016/j.prostr.2020.06.002
Saxena, A., 2019. Challenges in predicting crack growth in structures operating in extreme environments. Procedia Structural Integrity, SICE 2018 (2nd International Conference on Structural Integrity and Exhibition 2018) 14, 774–781. https://doi.org/10.1016/j.prostr.2019.07.055
Sreebunpeng, K., Chewpraditkul, W., Nikl, M., 2017. Light yield and light loss coefficient of LuAG:Ce and LuAG:Pr under excitation with α- and γ-rays. Journal of Crystal Growth, The 18th International Conference on Crystal Growth and Epitaxy (ICCGE-18) 468, 373–375. https://doi.org/10.1016/j.jcrysgro.2016.10.022
Swiderski, L., Moszynski, M., Nassalski, A., Syntfeld-Kazuch, A., Szczesniak, T., Kamada, K., Tsutsumi, K., Usuki, Y., Yanagida, T., Yoshikawa, A., Chewpraditkul, W., Pomorski, M., 2009. Scintillation Properties of Praseodymium Doped LuAG Scintillator Compared to Cerium Doped LuAG, LSO and $LaBr_3$. IEEE Transactions on Nuclear Science 56, 2499–2505. https://doi.org/10.1109/TNS.2009.2025040
Wang, J., Yang, Jinghan, Hu, T., Chen, X., Lang, J., Wu, X., Zhang, J., Zhao, H., Yang, Jinghai, Cui, Q., 2018. Structural Phase Transition and Compressibility of CaF_2 Nanocrystals under High Pressure. Crystals 8, 199. https://doi.org/10.3390/cryst8050199
Witkiewicz-Lukaszek, S., Gorbenko, V., Zorenko, T., Paprocki, K., Sidletskiy, O., Gerasymov, I., Mares, J.A., Kucerkova, R., Nikl, M., Zorenko, Y., 2018. Novel All-Solid-State Composite Scintillators Based on the Epitaxial Structures of LuAG Garnet Doped With Pr, Sc, and Ce Ions. IEEE Transactions on Nuclear Science 65, 2114–2119. https://doi.org/10.1109/TNS.2018.2838333
Xiang, R., Liang, X., Li, P., Di, X., Xiang, W., 2016. A thermally stable warm WLED obtained by screen-printing a red phosphor layer on the $LuAG:Ce^{3+}$ PiG substrate. Chemical Engineering Journal 306, 858–865. https://doi.org/10.1016/j.cej.2016.08.008
Xu, J., Wang, J., Gong, Y., Ruan, X., Liu, Z., Hu, B., Liu, B., Li, H., Wang, X., Du, B., 2018. Investigation of an LuAG:Ce translucent ceramic synthesized via spark plasma sintering: Towards a facile synthetic route, robust thermal performance, and high-power solid state laser lighting. Journal of the European Ceramic Society 38, 343–347. https://doi.org/10.1016/j.jeurceramsoc.2017.07.036
Yanagida, T., Fujimoto, Y., Kurosawa, S., Kamada, K., Takahashi, H., Fukazawa, Y., Nikl, M., Chani, V., 2013. Temperature Dependence of Scintillation Properties of Bright Oxide Scintillators for Well-Logging. Jpn. J. Appl. Phys. 52, 076401. https://doi.org/10.7567/JJAP.52.076401
Yang, H., Peng, F., Zhang, Q., Guo, C., Shi, C., Liu, W., Sun, G., Zhao, Y., Zhang, D., Sun, D., Yin, S., Gu, M., Mao, R., 2014. A promising high-density scintillator of $GdTaO_4$ single crystal. CrystEngComm 16, 2480–2485. https://doi.org/10.1039/C3CE42350F
Ziluei, H., Azimirad, R., Mojtahedzadeh Larijani, M., Ziaie, F., 2017. Preparation and optimization of $CdWO_4$-polymer nano-composite film as an alpha particle counter. Nuclear Instruments and Methods in Physics Research Section A: Accelerators, Spectrometers, Detectors and Associated Equipment 852, 85–90. https://doi.org/10.1016/j.nima.2017.01.015
Zorenko, Y., Douissard, P.-A., Martin, T., Riva, F., Gorbenko, V., Zorenko, T., Paprocki, K., Iskalieva, A., Witkiewicz, S., Fedorov, A., Bilski, P., Twardak, A., 2017. Scintillating screens based on the LPE grown $Tb_3Al_5O_{12}$:Ce single crystalline films. Optical Materials, Special Issue of the 7th International Symposium on Optical Materials (IS-OM7) 65, 73–81. https://doi.org/10.1016/j.optmat.2016.09.066